Structural Dynamics of Green Fluorescent Protein Alone and Fused with a Single Chain Fv Protein*

Mark A. Hink‡, Remko A. Griep§, Jan Willem Borst‡§, Arie van Hoek‡, Michel H. M. Eppink‡, Arjen Schots§, and Antonie J. W. G. Visser‡¶

From the ‡MicroSpectroscopy Centre, Department of Biomolecular Sciences and the §Laboratory for Monoclonal Antibodies, Department of Plant Sciences, Wageningen University, 6703 HA Wageningen, The Netherlands

Structural information on intracellular fusions of the green fluorescent protein (GFP) of the jellyfish *Aequorea victoria* with endogenous proteins is required as they are increasingly used in cell biology and biochemistry. We have investigated the dynamic properties of GFP alone and fused to a single chain antibody raised against lipopolysaccharide of the outer cell wall of Gram-negative bacteria (abbreviated as scFv-GFP). The scFv moiety was functional as was proven in binding assays, which involved the use of both fluorescence correlation spectroscopy observing the binding of scFv-GFP to Gram-negative bacteria and a surface plasmon resonance cell containing adsorbed lipopolysaccharide antigen. The rotational motion of scFv-GFP has been investigated with time-resolved fluorescence anisotropy. However, the rotational correlation time of scFv-GFP is too short to account for globular rotation of the whole protein. This result can only be explained by assuming a fast hinge motion between the two fused proteins. A modeled structure of scFv-GFP supports this observation.

The green fluorescent protein (GFP)[1] from the jellyfish *Aequorea victoria* has received widespread utilization as a natural fluorescent marker for gene expression, localization of gene products (1–5), and identification of protein interaction and function. GFP is a protein consisting of 238 amino acids with a molecular mass of 27 kDa and has the shape of a cylinder with a length of 4.2 nm and diameter of 2.4 nm. The chemical structure of the hexapeptide chromophore has been elucidated (6). The intrinsic fluorophore is a *p*-hydroxybenzylidene-imidazolidine derivative formed by a covalent modification of the sequence Ser[65] (or Thr[65] in enhanced GFP), Tyr[66], and Gly[67] in the hexapeptide. A comprehensive review on GFP has been published (7). The crystal structure of GFP and enhanced GFP has been solved and showed the hexapeptide to be part of a central helix inside a 11-stranded β-barrel (8–11).

Genetic fusions of a variety of proteins with GFP have been used in numerous studies on gene or protein function. In a sense it is miraculous that in most fusion proteins GFP is functional. In many other fusion proteins, the protein used as a reporter does often not fold well, resulting in aggregates or inclusion bodies of the entire fusion protein. Sometimes the causes of aggregation can be attributed to certain (clusters of) amino acids such as hydrophobic clusters of amino acids that become solvent exposed (12). To obtain a better picture why these phenomena do not occur in GFP fusion proteins, we have investigated the behavior of the GFP moiety in fusion proteins and emphasized the motional properties. Thereto, we fused enhanced GFP with a single chain Fv fragment raised against the lipopolysaccharide (LPS) of a Gram-negative bacterium. Because the single chain antibody was linked to the N-terminal residue of GFP, the fusion protein is abbreviated as scFv-GFP.

Here we report information relevant for the dynamics of GFP fusion proteins used to monitor protein function in both *in vitro* and *in vivo* biological systems. Fluorescence correlation spectroscopy (FCS) was used to measure the translational diffusion of GFP fusion proteins alone and to visualize the interaction of the scFv-GFP fusion with a much larger ligand (*i.e.* Gram-negative bacteria), having a much slower translation diffusion. In addition, rotational motion of the GFP part of scFv-GFP was studied with time-resolved fluorescence anisotropy. Both techniques were then used to characterize the motional dynamics of the GFP fusion construct. To obtain additional support for the observed rapid rotation of scFv-GFP, a structural model was built. The incentive to present the structure was to demonstrate that the two proteins are separated from each other by a flexible hinge allowing free motion and no mutual interference.

EXPERIMENTAL PROCEDURES

Materials—To change the fluorescence excitation peak of wild type green fluorescent protein from 396 to 488 nm (13), two amino acid changes (F64L and S65T) were introduced into the wild type GFP (14) by polymerase chain reaction. The GFP gene was ligated in frame with the scFv (with three alanine residues as linker). The produced GFP-mut1 protein was isolated and purified as described (15). The purity of GFP and scFv-GFP was assessed by SDS-polyacrylamide gel electrophoresis and Western blotting. Bacteria were plated on growth factor agar and treated with NaN$_3$ before the measurement. *Spodoptera frugiperda* insect cells (*Sf*21) were grown in Grace's insect medium (Sigma) containing 10% fetal calf serum and released from the culture flask bottom. Cell suspensions were diluted to a final concentration of 10^7 cells ml^{-1} using 0.1 M Tris-HCl buffer, pH 7.5, containing 0.01% Tween-80 and incubated with scFv-GFP at room temperature for 5 min.

Structural Model of scFv-GFP—To obtain a realistic impression of the structure of the scFv-GFP fusion product, a putative homology model was constructed. Structural models of the variable domains of the heavy (V$_H$) and light (V$_L$) chains of anti-LPS were derived by homology modeling using the AbM software package (version 2.0, Oxford Molecular). The best templates for the V$_L$ domain were the V$_L$ domains with Protein Data Bank code 1BAF (16) and 1BBD (17), both with 47% sequence identity. The best template for the V$_H$ domain of

¶ To whom correspondence should be addressed: MicroSpectroscopy Centre, Dept. of Biomolecular Sciences, Lab. of Biochemistry, Wageningen University, Dreijenlaan 3, 6703 HA Wageningen, The Netherlands. Fax: 31-317-484801; E-mail: Ton.Visser@laser.bc. wau.nl.

[1] The abbreviations used are: GFP, green fluorescent protein; FCS, fluorescence correlation spectroscopy; LPS, lipopolysaccharide; scFv, single chain fragment of the antibody variable domains.

anti-LPS was the V_H domain with Protein Data Bank code 1FVC (18) having 70% sequence identity. Both V_H and V_L domains of the homology models were together superimposed onto the V_H and V_L domains of 1BAF with the InsightII package (Release 97.0, Biosym Technologies, Inc.). The structure of GFP 1EMA (8) was obtained from the Protein Data Bank and the F64L mutation was introduced with the homology module of InsightII. The N terminus of the GFP molecule was coupled to the C terminus of the V_L domain with a linker of three alanines using the InsightII software. Because the overall structure will not be altered by solvation, no solvent molecules were included. The constructed scFv-GFP model was energy minimized with the conjugate gradient method of the XPLOR package (19) using the parameter set as determined by Engh and Huber (20). For the chromophoric group a topology and parameter set were generated with the XPLO2D program (21). The final model was obtained after 250 minimization cycles (gradient, 0.1 kcal/mol). The scFv-GFP model was stereochemical verified with PRO-CHECK (22), and the protein folding was assessed with PROSAII (23).

Analytical Methods—The surface plasmon resonance (24) experiments were performed with the BIAcore system (Amersham Pharmacia Biotech). Thereto, a streptavidin-coated sensorchip (Amersham Phar-

macia Biotech) was incubated with biotinylated lipopolysaccharide antigen. The experiments were performed like described in Kamiuchi *et al.* (25). The fluorescence correlation spectroscopic measurements were carried out with a Zeiss-Evotec ConfoCor® system using the 488-nm Ar ion laser line for excitation and the fluorescein emission filter set (maximum transmission between 530 and 570 nm). The concentration of scFv-GFP amounted to 6.0 nM by diluting with 0.1 M Tris-HCl buffer, pH 7.5. The autocorrelation curves were acquired during 20 s. The principle and experimental realization of FCS have been outlined in several recent papers (26–30). FCS data were analyzed with nonlinear least squares fitting of the parameters in the autocorrelation function describing diffusion in a three-dimensional Gaussian-shaped volume element with radii ω_{xy} and ω_z (e^{-2} intensity points of the Gaussian beam; the subscripts xy and z refer to the equatorial and axial radius, respectively):

$$G(t) = 1 + \frac{1}{N}\left(\frac{1}{1+\frac{t}{\tau_d}}\right)\sqrt{\left(\frac{1}{1+\frac{t}{a^2\tau_d}}\right)} \qquad \text{(Eq. 1)}$$

Here N denotes the number of fluorescent particles, a is equal to ω_z/ω_{xy}, and τ_d is the diffusion time of the fluorescent particle, which is related to the translational diffusion constant D_{trans}.

$$D_{trans} = \frac{\omega_{xy}^2}{4\tau_d} \qquad \text{(Eq. 2)}$$

N and τ_d are the parameters to be recovered, whereas the value for a is obtained by measuring the diffusion of an aqueous solution of 50 nM rhodamine 6G under identical experimental conditions. a was fixed in fitting the data according to Equation 1. Typical values determined were $\omega_{xy} = 0.248$ μm and $a = 7.6$. Because we have noted that the measured diffusion time of GFP was distinctly shorter upon the use of relatively high laser power (31), the FCS data were obtained with a relatively small laser power density of $\sim$20 kW cm^{-2}. The average hydrodynamic radius R_h of the protein can be obtained from the following equation.

$$R_h = \frac{kT}{6\pi\eta D_{trans}} \qquad \text{(Eq. 3)}$$

Time-resolved polarized fluorescence experiments were carried out using a picosecond laser system and time-correlated single photon counting as described in detail elsewhere (32–34). The excitation wavelength was 480 nm (coumarin 150 dye as laser medium, pumped by a mode-locked Nd-YLF laser), and the fluorescence was selected by using a bandpass filter (K50) in conjunction with a GG495 cut-off filter (both filters were from Schott, Mainz, Germany). The total fluorescence decay and the fluorescence anisotropy decay were analyzed using the global analysis program from Globals Unlimited, Inc. (Urbana, IL). The 67%
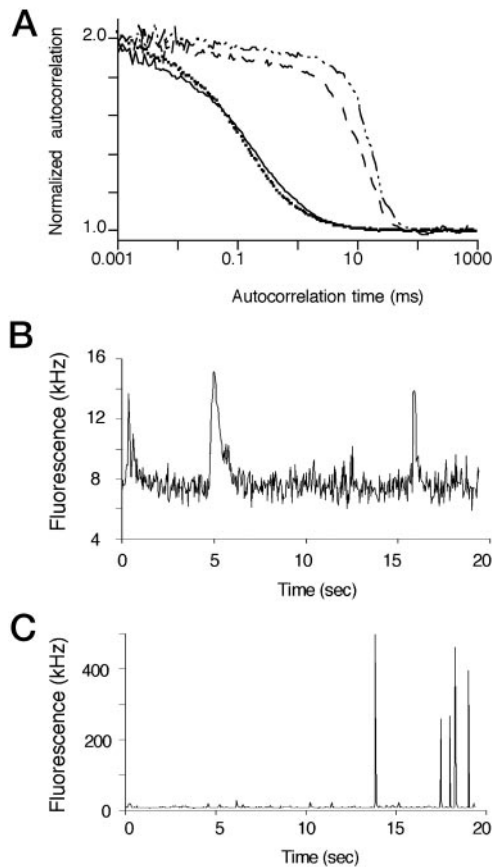
FIG. 1. **Binding of scFv-GFP to Gram-negative bacteria monitored with FCS.** *A*, the autocorrelation *curves* for scFv-GFP (*solid line*) and autofluorescent *R. solanacearum* bacteria (*dashed line*). Gram-positive (*dotted line*) and Gram-negative bacteria (*dashed* and *dotted line*) were incubated with scFv-GFP to monitor binding. All *curves* were scaled to 2.0 (equivalent to one molecule in the detection volume) for clarity. *B* and *C* show the fluorescence intensity *traces* of autofluorescent and immunolabeled bacteria, respectively.

TABLE I
Translational diffusion times and constants (τ_d, D_{trans}) and hydrodynamic radii (R_h) of green fluorescent protein and its fusion product to a single chain antibody (scFv-GFP)

The standard deviation mentioned at each parameter is obtained from 10 experiments (5 experiments for 2 different protein preparations). D_{trans} and R_h are calculated from Equations 2 and 3, respectively.

Sample	τ_d	D_{trans}	R_h
	μs	$(m^2\ s^{-1})\cdot 10^{11}$	nm
GFP	165 ± 4	9.32 ± 0.22	2.30 ± 0.05
scFv-GFP	254 ± 10	6.05 ± 0.24	3.54 ± 0.14

TABLE II
Fluorescence decay parameters (α_i, τ_i) and anisotropy decay parameters (β, ϕ, D_{rot}, R_h) of GFP and scFv-GFP

Values in parentheses with lifetimes and correlation times are the limiting values obtained after an exhaustive error search (at the 67% confidence limit) in a global analysis of two separate experiments. Pre-exponential factors are the average of two determinations and are accurate to the given digit (for instance, 0.37 indicates 0.37 ± 0.01).

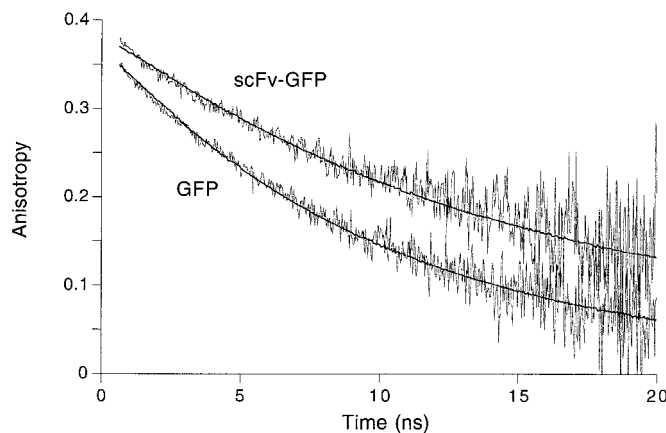| Sample	Fluorescence						Anisotropy		
	α_1	τ_1	α_2	τ_2	α_3	τ_3	β	ϕ	R_h
		ns		ns		ns		ns	nm
GFP	0.23	0.51 (0.43–0.58)	0.70	2.57 (2.48–2.65)	0.07	4.9 (4.6–5.4)	0.37	10.6 (10.2–11.0)	2.21 (2.18–2.23)
scFv-GFP	0.21	0.53 (0.45–0.60)	0.73	2.53 (2.40–2.61)	0.06	4.1 (3.5–5.0)	0.38	15.8 (14.9–16.5)	2.52 (2.47–2.56)

FIG. 2. **Fluorescence anisotropy decay curves of GFP and scFv-GFP.** The experimental curves (noisy curves) were fitted with a single correlation time of 10.8 ns for GFP and of 15.8 ns for scFv-GFP (*solid lines*). Full results of analysis are collected in Table II.

confidence limits of fluorescence lifetimes and rotational correlation times were determined in a rigorous error analysis by linking two experiments on two different protein preparations. The hydrodynamical radius of the particles (R_h) could be calculated from the rotational correlation time (ϕ) via the Debye-Stokes-Einstein equation.

$$R_h = \sqrt[3]{\frac{3\phi kT}{4\pi\eta}} \qquad \text{(Eq. 4)}$$

where T is the temperature (K) and η is the viscosity of water. The GFP concentration used was 200 nM adjusted with 0.1 M Tris-HCl buffer at pH 7.5. The same buffer was used to obtain a scFv-GFP concentration of 80 nM. The temperature of all experiments was 295 K.

RESULTS AND DISCUSSION

Diffusion and Binding—To assess whether or not the genetic fusion of GFP to a single chain Fv alters the binding properties, the affinity for LPS of scFv alone and fused with GFP was measured using surface plasmon resonance measurements. The measured affinities of 0.92 nM for the scFv alone and 1.0 nM for the scFv-GFP fusion protein can be considered as identical because the discrepancy falls within the experimental error.

FCS experiments were performed to test the binding of scFv-GFP to the outer membrane of Gram-negative bacteria, rich in LPS. This should result in a large fluorescent complex with a significantly longer diffusion time compared with the relatively small, unbound scFv-GFP. In Fig. 1*A* a typical autocorrelation curve for scFv-GFP is presented resulting in a diffusion time of 256 μs. Incubation with *Ralstonia solanacearum* (Gram-negative) bacteria resulted in a large increase of the diffusion time to 45 $\pm$ 21 ms (*dotted line*), indicating the presence of large, slowly diffusing complexes. The diffusion time had a similar value as that of the nonlabeled autofluorescent bacteria (38 $\pm$ 18 ms) (*dashed line*), because binding of the relatively small scFv-GFP would hardly increase the radii of the bacterial cells. However, because immunolabeled cells (Fig. 1*C*) were almost 40 times more fluorescent than the autofluorescent bacterial cells (Fig. 1*B*), both cell types could be distinguished from each other. In a control experiment, Gram-positive bacteria (*C. histolyticum*) or *Sf*21 insect cells were added to a scFv-GFP solution. In both cases the diffusion time was approximately 260 μs, and no high intensity peaks in the fluorescent traces were found, indicating that no immunolabeled cells were present (Fig. 1*A*, *dotted line*). From the FCS experiments on scFv-GFP alone, a translational diffusion constant (D_{trans}) of 6.05 $\pm$ 0.24 $\times$ 10^{-11} m^2 s^{-1} was calculated, which corresponds to a particle with an apparent hydrodynamic radius of 3.54 nm. The translational diffusion coefficient of GFP alone is $D_{trans} = $ 9.32 $\times$ 10^{-11} m^2 s^{-1}. R_h turns out to be 2.30 nm (Table I).

Another report on FCS on wild type GFP mentioned a value of $D_{trans} = 8.7 \times 10^{-11}$ m^2 s^{-1} yielding a Stokes radius of 2.82 nm (35). In the latter publication the concentrations used were much higher (in the order of 200 nM), and the number of particles in the confocal volume element amounted to 120 and 240, giving rise to a much lower amplitude of the autocorrelation function than obtained in this work. The translational diffusion coefficient reported in Ref. 35 is therefore less precisely determined. Diffusion coefficients of the GFP mutant S65T have also been obtained from experiments of fluorescence recovery after photobleaching (36). The latter authors came to a similar value of D_{trans} as reported in Ref. 35. However, the GFP concentration used in that work was 30 μM, which is 4 orders of a magnitude higher than in our experiments.

Time-resolved Fluorescence and Rotation—Time-resolved polarized fluorescence of GFP also results in an average hydrodynamic radius and indicates that the chromophoric group rotates together with the protein. Three fluorescence lifetimes were needed to give an optimal fit. These lifetime components and pre-exponential factors are collected in Table II. The main fluorescence lifetime is 2.6 ns, in fair agreement with values obtained previously, but lifetimes of 0.50 and 4.9 ns are also present. The heterogeneity of the fluorescence decay is consistent with the reaction scheme proposed previously from subpicosecond time-resolved fluorescence spectroscopy (37–39). This scheme has taken into account equilibria between different ground and excited states, proton transfer, and photoconversion processes. These multiple states and the interconversion between them would lead to an inherent nonexponential decay as observed. The fluorescence anisotropy decay analysis of GFP yields a single rotational correlation time ϕ of 10.6 ns (Table II and Fig. 2). The fluorophore is rigidly bound in the protein matrix and rotates together with the whole protein. This observation is in full agreement with the three-dimensional structures in which the fluorophore is rigidly incorporated in the central helix (8–10). The rigidity of the binding site seems a general property of fluorophores involved in bioluminescence; there is no internal motion of other light emitting antenna fluorophores as well (34, 40). The hydrodynamic radius (R_h) calculated from the obtained rotational correlation time (Equation 4) is 2.21 nm (Table II) and in good agreement with the fluorescence correlation experiment.

The fluorescence decay of scFv-GFP contains the same lifetime components as those arising from GFP alone (Table II). However, the fluorescence anisotropy decays more rapidly than can be expected for a fusion product, which is about twice the size of a single GFP molecule (Fig. 2). For globular proteins the rotational correlation time is proportional to the molecular mass. Therefore, it is expected that the correlation time is longer than 20 ns, when the two fused proteins are rotating as one unit. The reason for the shorter correlation time should be sought in the flexibility of the peptide region linking the two proteins. The transport properties of macromolecules with segmental flexibility have been theoretically investigated via simulations of the fluorescence anisotropy decay for two rigid proteins connected by a flexible hinge (41, 42). It was shown that segmental flexibility is detected by fluorescence anisotropy provided that the orientation of the emission transition dipole is such that it reports on the bending motion. On the other hand, the dipole can also be wrongly oriented so that the anisotropy decay is like that of a rigid body, and no flexibility will be observed. Another important outcome of these simulations is that the extent of bending cannot be inferred from a two-exponential fit to the anisotropy decay. Apparently in our case of scFv-GFP the emission transition dipole of GFP has a favorable geometry for sampling the flexibility of the hinge between
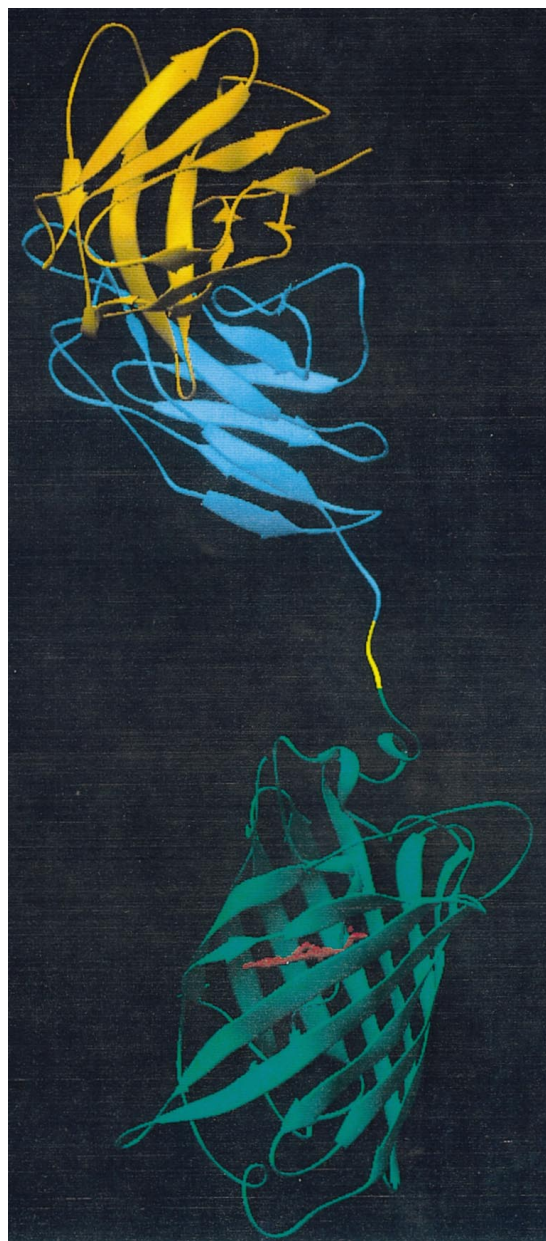
between GFP and the variable fragment of the light chain consists of three alanine residues. Together with the three C-terminal amino acids of the light chain, a flexible connection between GFP and the single chain antibody is formed, well separating both proteins. This observation fully agrees with the data obtained with time-resolved fluorescence anisotropy, where a flexible hinge between two rigid fragments can explain the relatively short rotational correlation time. The structure also explains that the scFv-GFP construct easily recognizes its antigen. There is no spatial interference between the two proteins, and the antigen-binding site is fully exposed. It can be anticipated that the same applies to most other GFP fusion proteins and as such accounts for the success of this reporter protein.

REFERENCES

1. Heim, R., Prasher, D. C., and Tsien, R. Y. (1994) *Proc. Natl. Acad. Sci. U. S. A.* **91,** 12501–12504
2. Chalfie, M., Tu, Y., Euskirchen, G., Ward, W., and Prasher, D. (1994) *Science* **263,** 802–805
3. Heim, R., Cubitt, A., and Tsien, R. Y. (1995) *Nature* **373,** 663–664
4. Heim, R., and Tsien, R. Y. (1996) *Curr. Biol.* **6,** 178–182
5. Delagrave, S., Hawtin, R. E., Silva, C. M., Yang, M. M., and Youvan, D. C. (1995) *Bio/Technology* **13,** 151–154
6. Cody, C. W., Prasher, D. C., Westler, W. M., Prendergast, F. G., and Ward, W. W (1993) *Biochemistry* **32,** 1212–1218
7. Tsien, R. Y. (1998) *Annu. Rev. Biochem.* **67,** 509–544
8. Ormö, M., Cubitt, A. B., Kallio, K., Gross, L. A., Tsien, R. Y., and Remington, S. J. (1996) *Science* **273,** 1392–1395
9. Yang, F., Moss, L. G., and Phillips, G. N. (1996) *Nat. Biotechnol.* **14,** 1246–1251
10. Brejc, K., Sixma, T. K., Kitts, P. A., Kain, S. R., Tsien, R. Y., Ormö, M., and Remington, S. J. (1997) *Proc. Natl. Acad. Sci. U. S. A.* **94,** 2306–2311
11. Elsiger, M. A., Wachter, R. M., Kallio, K., Hanson, G. T., and Remington, S. J. (1999) *Biochemistry* **38,** 5296–5301
12. Wall, J. G., and Plückthun, A. (1999) *Prot. Eng.* **12,** 605–611
13. Cormack, B. P., Valdivia, R., and Falkow, S. (1996) *Gene (Amst.)* **173,** 33–38
14. Prasher, D. C, Eckenrode, V. K., Ward, W. W., Prendergast, F. G., and Cormier, M. J. (1992) *Gene (Amst.)* **111,** 229–233
15. Griep, R. A., van Twisk, C., van Beckhoven, J. K. C. M., van der Wolf, J. M., and Schots, A. (1998) *Phytopathology* **88,** 795–803
16. Brünger, A. T, Leahy, D. J., Hynes, T. R., and Fox, R. O. (1991) *J. Mol. Biol.* **221,** 239–256
17. Tormo, J., Stadler, E., Skern, T., Auer, H., Kanzler, O., Betzel, C., Blaas, D., and Fita, I. (1993) *Protein Sci.* **1,** 1154–1161
18. Eigenbrot, C., Randal, M., Presta, L., Carter, P., and Kossiakoff, A. A. (1993) *J. Mol. Biol.* **229,** 969–995
19. Brünger, A. T. (1992) *X-PLOR*, version 3.1, Yale University Press, New Haven, CT
20. Engh, R. A., and Huber, R. (1991) *Acta Crystallogr. Sect. A* **47,** 392–400
21. Kleywegt, G. J. (1995) *ESF/CCP4 Newsletter* **31,** 45–50
22. Laskowski, R. A., MacArthur, M. W., Moss, D. S., and Thornton, J. M. (1993) *J. Appl. Crystallogr.* **26,** 283–291
23. Sippl, M. J. (1993) *Proteins* **17,** 355–362
24. Kretschmann, E., and Raether, H. (1968) *Z. Naturforsch.* **23,** 2135–2136
25. Kamiuchi, T., Abe, E., Imanishi, M., Kaji, T., Nagaoka, M., and Sugiura, Y. (1998) *Biochemistry* **37,** 13827–13834
26. Thompson, N. L. (1991) in *Topics in Fluorescence Spectroscopy* (Lakowicz, J. R., ed) Vol. 1, pp. 337–378, Plenum Press, New York
27. Rigler, R., Widengren, J., and Mets, Ü. (1993) in *Fluorescence Spectroscopy. New Methods and Applications* (Wolfbeis, O. S., ed) pp. 13–24, Springer Verlag, Berlin
28. Eigen, M., and Rigler, R. (1994) *Proc. Natl. Acad. Sci. U. S. A.* **91,** 5740–5747
29. Maiti, S., Haupts, H., and Webb, W. W. (1997) *Proc. Natl. Acad. Sci. U. S. A.* **94,** 11753–11757
30. Hink, M. A., van Hoek, A., and Visser, A. J. W. G. (1999) *Langmuir* **15,** 992–997
31. Visser, A. J. W. G., and Hink, M. A. (1999) *J. Fluorescence* **9,** 81–87
32. Leenders, R., Kooijman, M., van Hoek, A., Veeger, C., and Visser, A. J. W. G. (1993) *Eur. J. Biochem.* **211,** 37–45
33. van Hoek, A., and Visser, A. J. W. G. (1992) *Proc. SPIE* **1640,** 325–329
34. Visser, A. J. W. G., van Hoek, A, Visser, N. V., Lee, Y., and Ghisla, S. (1997) *Photochem. Photobiol.* **65,** 570–575
35. Terry, B. R., Matthews, E. K., and Haseloff, J. (1995) *Biochem. Biophys. Res. Commun.* **217,** 21–27
36. Swaminathan, R., Hoang, C. P., and Verkman, A. S. (1997) *Biophys. J.* **72,** 1900–1907
37. Lossau, H., Kummer, A., Heinecke, R., Pöllinger-Dammer, F., Kompa, C., Bieser, G., Jonsson, T., Silva, C. M., Yang, M. M., Youvan, D. C., and Michel-Beyerle, M. E. (1996) *Chem. Phys.* **213,** 1–16
38. Beechem, J. M., Gratton, E., Ameloot, M., Knutson, J. R and Brand, L. (1992)

FIG. 3. **Ribbon drawing of the Cα backbone of the scFv-GFP model.** The GFP is shown in *green*, the variable light domain is in *blue*, the variable heavy domain is in *orange*, the linker region is in *yellow*, and the chromophoric group is in *red*. This schematic ribbon diagram was generated with RIBBONS (48).

two relatively rigid molecules. Also in line with the simulations (42) is the fact that the fluorescence anisotropy decay is a single exponential.

Biological Significance—GFP has been fused successfully as a reporter protein to many different proteins in both *in vivo* and *in vitro* experiments (see for instance Refs. 43–47). Many of these reports account to revealing the biological function of proteins. The results presented here explain why the use of GFP is so often successful. It was found that both fusion partners behaved independently, in a fashion identical to the "parent" protein. This is an important finding because it shows that GFP does not influence the biological behavior of its fusion partner and that, *vice versa*, GFP is not very sensitive to influences of other proteins fused with it. To visualize this, a structural model of the scFv-GFP construct used in this study was made. The Cα backbone is presented in Fig. 3. The linkage

Topics in Fluorescence Spectroscopy (Lakowicz, J. R., ed) Vol. 2, pp. 241–305, Plenum Press, New York
39. Chattoraj, M., King, B. A., Bublitz, G. U., and Boxer, S. G. (1996) *Proc. Natl. Acad. Sci. U. S. A.* **93,** 8362–8367
40. Lee, J., Matheson, I. B. C., Müller, F., O'Kane, D. J., Vervoort, J., and Visser, A. J. W. G. (1991) *Chemistry and Biochemistry of Flavoenzymes* (Müller, F., ed) Vol. 2, pp. 109–151, CRC Press, Boca Raton, FL
41. Harvey, S. C. (1979) *Biopolymers* **18,** 1081–1104
42. Harvey, S. C., and Cheung, H. C. (1980) *Biopolymers* **19,** 913–930
43. Haraguchi, T., Ding, D. Q., Yamamoto, A., Kaneda, T., Koujin, T., and Hiraoka, Y. (1999) *Cell Struct. Funct.* **24,** 291–298
44. McLean, A. J., Bevan, N., Rees, S., and Milligan, G. (1999) *Mol. Pharmacol.* **56,** 1182–1191
45. Walker, D., Htun, H., and Hager, G. L. (1999) *Methods Companion Methods Enzymol.* **19,** 386–393
46. Otsuki, M., Fukami, K., Kohno, T., Yokota, J., and Takenawa, T. (1999) *Biochem. Biophys. Res. Commun.* **266,** 97–103
47. Zhu, H. Y., Yamada, H., Jiang, Y. M., Yamada, M., and Nishiyama, Y. (1999) *Arch. Virol.* **144,** 1923–1935
48. Carson, M. C. (1991) *J. Appl. Crystallogr.* **24,** 958–961